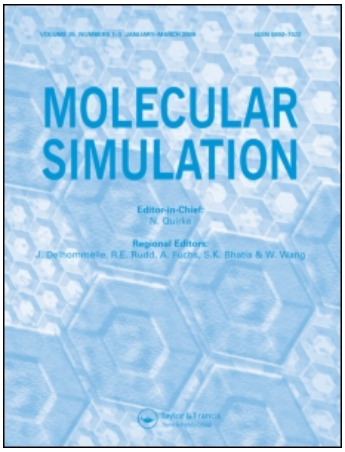

Molecular Simulation
Publication details, including instructions for authors and subscription information:
http://www.informaworld.com/smpp/title~content=t713644482

Potential optimization for the calculation of shocked liquid nitromethane properties

N. Desbiens[a]; E. Bourasseau[a]; J. -B. Maillet[a]
[a] CEA, Département de Physique Théorique et Appliquée, Bruyères-le-Châtel, France

First published on: 13 September 2007

To cite this Article Desbiens, N. , Bourasseau, E. and Maillet, J. -B.(2007) 'Potential optimization for the calculation of shocked liquid nitromethane properties', Molecular Simulation, 33: 13, 1061 — 1070, First published on: 13 September 2007 (iFirst)
To link to this Article: DOI: 10.1080/08927020701589245
URL: http://dx.doi.org/10.1080/08927020701589245

Molecular Simulation, Vol. 33, No. 13, November 2007, 1061–1070

Taylor & Francis
Taylor & Francis Group

Potential optimization for the calculation of shocked liquid nitromethane properties

N. DESBIENS, E. BOURASSEAU and J.-B. MAILLET*

CEA, Département de Physique Théorique et Appliquée, BP12, 91680 Bruyères-le-Châtel, France

(Received May 2007; in final form July 2007)

We present the results of the optimization of a classical molecular force field used to calculate the properties of shocked nitromethane by Monte Carlo simulations. The optimization technique allows a good transferability of the potential parameters on a broad range of thermodynamic conditions (temperature and pressure) since a large variety of reference data can be used in the optimization procedure, including densities, vaporization enthalpies or pressures along the Hugoniot curve. Results of calculated properties of shocked nitromethane are in good agreement with experimental shock Hugoniot data, including temperature measurements of second shock Hugoniot.

Keywords: Parameter optimization; Nitromethane; Shock Hugoniot; Monte Carlo simulations

1. Introduction

Understanding behavior of shocked materials still remains a challenge of current research capabilities. Experimental devices come to a point where microscopic information can directly be investigated and compared to "computer experiments", i.e. molecular simulations of the same material. This enhances the need for an accurate description of complex materials at the microscopic scale. We focus here on thermodynamic and structural properties of liquid nitromethane along its Hugoniot curve, which still remains poorly described, despite the fact that nitromethane is one of the most studied organic explosive, both experimentally [1,2] and by simulation [3–5]. Since we aim at obtaining the Hugoniot curve of complex systems, only classical molecular simulations can be considered. *Ab initio* methods are too much time consuming to provide us with informations on Hugoniot of explosives such as nitromethane. Molecular simulations are based on an atomic description of matter. As a consequence, the accurate calculation of structural and thermodynamic properties depends on the capability of the potential to describe intermolecular and intramolecular interactions. This is usually well done in standard conditions due to the fact that potentials are adjusted over experimental properties measured at low pressures and temperatures. The particularity of studying shocked properties of materials is the need of an accurate description of matter over a broad range of pressure and temperature. This can be achieved by using a robust potential, i.e. a potential which parameters are fitted on the basis of reference data taken at different densities or pressures. These types of potential are not usually available in the literature. This is why we proposed a specific procedure to fit potential parameters on a wide variety of thermodynamic data.

A classical force field is usually expressed as a sum of several independent contributions. These contributions are split on the basis of physical meaning: for example, intramolecular, intermolecular and electrostatic contributions. Following the ideas proposed by Bourasseau and coworkers in previous works [6–8], we develop a general method to obtain realistic and robust parameters. This method follows three points [9]. First, the functional form of the potential should be compatible with the classical picture of a molecular material such that each contribution to the potential could eventually be fitted separately. Secondly, the reference database should be chosen carefully. This is determinant for the subsequent robustness of the potential. Finally, the minimization

*Corresponding author. Email: nicolas.desbiens@cea.fr

Molecular Simulation
ISSN 0892-7022 print/ISSN 1029-0435 online © 2007 Taylor & Francis
http://www.tandf.co.uk/journals
DOI: 10.1080/08927020701589245

routine should be chosen accordingly to the optimization problem. A single parameter optimization over a small variation domain should refer to a different procedure than a ten parameters optimization over a broad range of variation. Whereas a systematic investigation can be envisaged in the former case, a random exploration of the parameter space is certainly more suited in the latter.

Details about the optimization procedure of the electrostatic contribution, applied to the potential of nitromethane and HF are given in [6,7]. Briefly, the charge equilibration method has been chosen to compute partial atomic charges on each atom [10,11]; indeed, this method has successfully been applied to hydrogen-bonded liquids such as water [12]. This method reproduces atomic charge changes with respect to local molecular environments. In the case of nitromethane, the parameters have been optimized to minimize the error function $F = F_{\text{charges}} + F_{\text{potential}}$. The expression of F_{charges} (respectively, $F_{\text{potential}}$) is reported in equation (1) (respectively, 2).

$$F_{\text{charges}} = \sum_{\text{conf}} \left[\frac{1}{N_{\text{at}} N_{\text{mol}}} \sum_{\text{at}} \sum_{\text{mol}} \left(\frac{q_{\text{at}}^{\text{calc}} - q_{\text{at}}^{\text{ref}}}{q_{\text{at}}^{\text{ref}}} \right)^2 \right], \quad (1)$$

where conf corresponds to the configurations used (4 in the case of nitromethane), $q_{\text{at}}^{\text{calc}}$ are the atomic partial charges calculated using the charge equilibration method and $q_{\text{at}}^{\text{ref}}$ are the atomic partial charges taken from a Bader analysis of several configurations of dense liquid [7].

$$F_{\text{potential}} = \sum_{\text{conf}} \left[\sqrt{ \frac{1}{N_{\text{elec}}} \sum_{i}^{N_{\text{elec}}} \left(\frac{V_i^{\text{calc}} - V_i^{\text{ref}} - C_{\text{conf}}}{V_{\text{tol}}} \right)^2 } \right] \quad (2)$$

N_{elec} points (around 100) have been randomly selected in these same configurations. Values taken by the electrostatic potential on these selected points (V_i) have been included in the error function. C_{conf} is a constant allowing the comparison of classical and *ab initio* results (see details in [6]).

We expose in this paper the second step of the optimization process of the potential of nitromethane consisting in choosing and fitting the repulsive and dispersive contributions.

Ideally, each contribution should be optimized separately, i.e. on specific reference data which depend only on the contribution itself [6–8]. A natural sequence of optimization then appears: both the intramolecular part and the electrostatic part can be optimized on specific reference data. They should be optimized first. Concerning the repulsive and dispersive part of the potential, to our knowledge, no specific data are available for the optimization. Then, global data, i.e. data that involve the whole potential, have to be used for the optimization process of this part of the potential. As a consequence, the optimized parameters will not only describe the "real" repulsive and dispersive interactions, but will also correct the non-avoidable error caused by the optimization of the first two contributions.

This paper is organized as follow. In Section 2 are reported the force field used and the properties of nitromethane with an initial potential parameter set. In Section 3, the error function used in the optimization procedure and the minimization procedure are detailed together with the optimized potential parameter set. Then, the thermodynamic and structural properties of nitromethane obtained with the optimized potential are compared to other published results for shocked nitromethane. A final comparison with experimental results is also provided on shocked and re-shocked nitromethane properties.

2. Force field and initial results

2.1. Force field

The first force field contribution that can be optimized is the intramolecular part. Along the Hugoniot curve, due to high pressure, the molecular structure could be modified. Nevertheless, the variations of bond lengths of nitromethane are limited to 3.5% [13]. In order to verify if those variations should be taken into account, we have constructed a rigid model molecule and have compared the Hugoniot curve calculated with a fixed molecular geometry to the same curve calculated using the modified molecular geometry. Results indicate that the small differences in bond length do not have a large influence on the Hugoniot curve. Similar conclusions can be drawn for the bond angles analysis. As a consequence, we chose to fix the internal geometry of the molecule. The chosen bond lengths and bond angles are reported in table 1. These values are taken from Ref. [14] except d_{CM}. *M* corresponds to the position of the centre of force for the methyl group and is placed on the CN axis towards the hydrogen atoms. The d_{CM} value is the Anisotropic United Atom displacement proposed by Ungerer *et al.* [15] for *n*-alkanes.

The second potential contribution to be optimized is the electrostatic part. The charge equilibration method has been applied to nitromethane [7] in order to compute the variation of charge with density and local environment. It appears that in the case of nitromethane (i.e. a liquid without hydrogen bonding), a fixed charge model remains a good approximation, the width of the charge distribution being relatively small. The values of the charges are chosen by using the average *ab initio* charges on N, O and

Table 1. Internal geometry of nitromethane.

Bond lengths & angle	
d_{NO}	1.225 Å [14]
d_{NC}	1.49 Å [14]
d_{CM}	0.21584 Å [14]
$\widehat{\text{ONO}}$	125.0° [15]

M calculated on different configurations of liquid nitromethane at 300 K between 0.9 and 1.6 g cm^{-3} [7].

Finally, concerning the repulsion interaction, as discussed by Liu *et al.* [16], a Lennard-Jones functional form does not seem to be appropriate to describe the short-range repulsion. At high pressures, the exp-6 functional form is known to be more suitable [17,18]. As a consequence, the exp-6 functional form has been chosen. The final functional form of the nitromethane potential remains quite simple: the molecule is modelled by four force centers located on the oxygen and nitrogen atoms and on the methyl group. Each force center has a partial charge and wears a exp-6 potential. The interaction energy between two force centers is then given by:

$$U(r_{ab}) = \frac{\varepsilon_{ab}}{\alpha_{ab} - 6}\left[6e^{\alpha_{ab}(1-((r_{ab})/(\sigma_{ab})))} - \alpha_{ab}\left(\frac{\sigma_{ab}}{r_{ab}}\right)^6\right] + \frac{q_a q_b e^2}{4\pi\varepsilon_0 r_{ab}} \tag{3}$$

The initial values of the potential parameters, i.e. before optimization, are given in table 2. The ε and σ parameters have been deduced from the Lennard-Jones parameters of nitrogen and oxygen atoms of nitromethane taken from [14]. The σ_M and ε_M have been deduced from Ref. [19] and are suited to the study of liquid–vapor equilibria of linear alkanes. The α parameters have been taken from the work of Sorescu *et al.* [20]. Standard mixing rules have been used and are reported in equation (4).

$$\sigma_{ab} = \frac{\sigma_a + \sigma_b}{2} \quad \varepsilon_{ab} = \sqrt{\varepsilon_a \varepsilon_b} \quad \alpha_{ab} = \sqrt{\alpha_a \alpha_b} \tag{4}$$

At last, the potential used describes only the inert molecule and chemical reactivity is not taken into account.

2.2. Hugoniot properties of nitromethane with the initial potential

The so-called Hugoniot curve is the ensemble of accessible states that a system can reach after a shock from an initial state. The thermodynamic quantities of a material in the initial unshocked state and the final shocked state are linked by the Hugoniot conservation relations of mass, momentum and energy:

$$\rho(u_s - u_p) = \rho_0 u_s \quad p - p_0 = \rho_0 u_s u_p$$

$$E - E_0 = \frac{1}{2}(p + p_0)(v_0 - v)$$

Table 2. Initial potential parameters of nitromethane.

	σ (Å)	ϵ (K)	α	q (e)
N	3.648	60.36	13.78944	+0.54
O	3.322488	85.51	13.157	−0.37
M	4.041	100	14.5476	+0.20

E is the internal energy per mass unit, p is the pressure, ρ is the density of the material and $v = 1/\rho$. The subscript "0" refers to the initial unshocked state. u_s is the shock velocity in the material and u_p is the particle velocity.

Using a constrain method to compute the Hugoniot curve implies the knowledge of the initial state of the material. In our case, the conditions of the initial state as given by the experiments are $P_0 = 1$ atm and $T_0 = 298$ K. In order to determine the specific volume V_0 and the energy U_0 of nitromethane in the initial state, a *NPT* simulation is performed over eight millions steps to ensure a good convergence, with a system of 150 molecules.

The obtained average density is 1135 ± 3 kg m^{-3} and the obtained vaporization enthalpy is 37.33 ± 0.09 kJ mol^{-1}, to be compared to experimental values of 1137 kg m^{-3} [21] and 38.271 kJ mol^{-1} [22], respectively. This corresponds to a difference of 0.2% for the density and 2.4% for the vaporization enthalpy.

In order to compute the Hugoniot curve of the system, we employed the Adaptive Erpenbeck—Equation of State (AE-EOS) method proposed by Brennan and Rice [23]. As discussed in this paper, it is possible to implement this method following several algorithms. We did not follow the idea of Brennan, who chose a succession of *NPT* simulations to converge to the Hugoniot pressure at a given temperature. Indeed the Hugoniot curve is usually plotted in either the (u_s, u_p)—shock velocity vs particle velocity—or (P, V) diagrams because it corresponds to direct observable of the system. The temperature is not a direct measure, and its calculation generally implies the use of particular approximations. In these conditions, temperature does not seem to be the most relevant quantity to use as a constrain. Instead, we proposed a way to implement the AE-EOS method based on a succession of *NVT* simulations [24,25]. In our simulations, the volume is constrained and the temperature is adjusted in order to fulfill the Hugoniot conditions. Finally, this method appears more efficient considering that *NVT* simulations converge more quickly than *NPT* simulations. Such simulations have been performed to compute Hugoniots of detonation products mixtures [25].

Starting from an initial configuration, the system is simulated in the canonical ensemble (NVT_1) and the following expression, corresponding to the Hugoniot difference $H_g(1)$ is evaluated by averaging over several hundred of thousand iterations:

$$H_g = E - E_0 - \frac{1}{2}(P + P_0)(V_0 - V) \tag{5}$$

The H_g term measures the gap between the simulated thermodynamic state and the real Hugoniot state.

After several hundred of thousand iterations (typically 500,000 in our case), the temperature of the simulation is slightly modified from T_1 to T_2 (± 10 K). During the following 500,000 iterations, $H_g(2)$ is evaluated. At the end of this second step, the following derivative is

evaluated:

$$\frac{\mathrm{d}H_g}{\mathrm{d}T}(2) = \frac{H_g(1) - H_g(2)}{T_1 - T_2} \tag{6}$$

From here, the new temperature of the simulation T_3 is calculated through:

$$T_3 = T_2 - \frac{H_g(2)}{((\mathrm{d}H_g)/(\mathrm{d}T))(2)} \tag{7}$$

and the simulations NVT_3 is performed for 500,000 iterations, during which $H_g(3)$ is evaluated.

This process is automatically iterated every 5×10^5 steps, evaluating each time:

$$\frac{\mathrm{d}H_g}{\mathrm{d}T}(n) = \frac{H_g(n-1) - H_g(n)}{T_{n-1} - T_n} \tag{8}$$

and a new temperature is calculated using:

$$T_{n+1} = T_n - \frac{H_g(n)}{((\mathrm{d}H_g)/(\mathrm{d}T))(n)} \tag{9}$$

Until the Hugoniot difference $H_g(n)$ has converged to the required accuracy. Once the Hugoniot temperature T_{hug} is reached, an additional NVT_{hug} simulation could be performed in order to compute accurately the pressure *Phug*. The advantage of this method is its rapidity. The convergence on the Hugoniot curve is usually obtained after 5×10^6 steps only performed in the *NVT* ensemble (this corresponds to 10 temperature changes).

Once the initial state is calculated, the whole Hugoniot curve can be simulated by AE-EOS NV_{hug} simulations. Each point on the Hugoniot curve is given by one simulation at a fixed value of V/V_0, so that only 6 simulations are sufficient to give a good idea of the Hugoniot curve. Other details can also be found in [24]. Our results are reported in figure 1. Other Hugoniot curves of nitromethane, based on Molecular dynamics simulations, have been reported in the litterature (figure 1). The results obtained by Jones [26] are in good agreement with the experiments while the one's of Liu [16] are markedly different. Soulard's results [27] and our own results are quite different from the experimental data. The difference is about 40% on the pressure at $V/V_o \sim 0.6$ from the experiments and underlines the need of potential optimization.

As stated above, the temperature does not appear as the most relevant parameter to constrain the system to satisfy the Hugoniot relation. Nevertheless, simulated shock temperatures remains a good indicator of the quality of a force field. The prediction of shock temperatures is an important issue in the studies of energetic materials. The results obtained by Soulard, Jones and Liu *et al.* are compared to our results and to the Lysne and Hardesty's results [1] (experimental results and physical equation of state) in figure 2. The temperatures obtained by MD simulations are lower than the ones of Lysne and Hardesty and the discrepancy

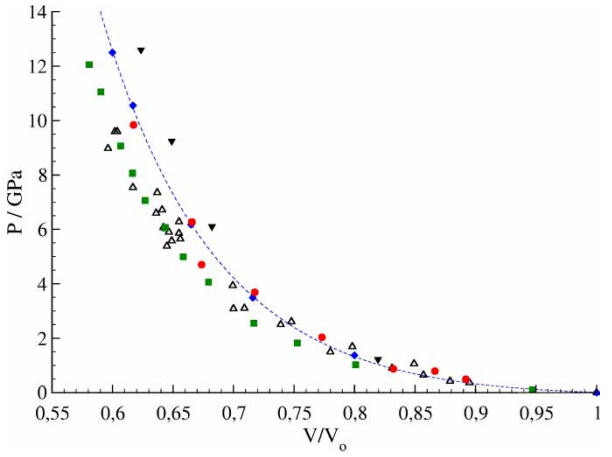

Figure 1. Hugoniot curves of nitromethane. Open triangles correspond to experimental data of Crouzet [28], Marsh [29], Klébert [30] and Craig [31]. Full symbols are results of simulations. Green squares: Jones [26], red dots: Soulard [27], black triangles down: Liu *et al.* [16] and blue losanges correspond to this work with the potential parameters reported in table 2. Dashed line is a guide to the eyes. (Colour in online version)

increases as the pressure increases. Our results are in better agreement with Lysne and Hardesty's results. Moreover, the slope of the curve is close to the experimental one, with a maximum difference of 80 K at 3.5 GPa.

The determination of the shock velocity (u_s) and particle velocity (u_p) from Monte Carlo molecular simulations is then performed by using the Rankine–Hugoniot relations. The $u_s(u_p)$ curve has been studied but not shown here because no major differences can be noticed between simulation results and experimental results. Our results and the results of Soulard, Jones and Liu *et al.* compare very well to Lysne and Hardesty's data.

The large discrepancies observed in the $(P - V)$ diagram led us to consider an optimization of the force field.

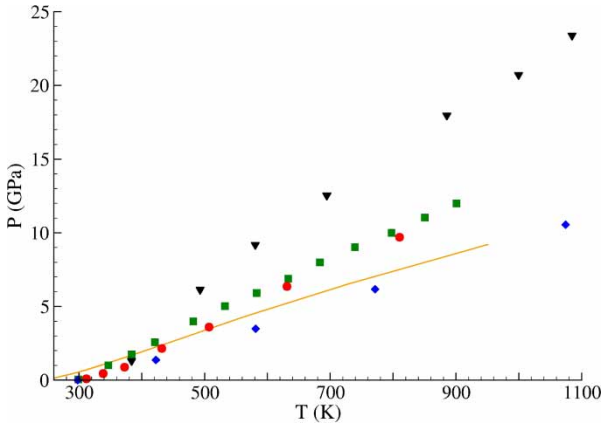

Figure 2. Pressure vs. temperature for the shock Hugoniot of nitromethane. Orange line: Lysne and Hardesty [1], Green squares: Jones [26], red dots: Soulard [27], black triangles down: Liu *et al.* [16] and blue losanges correspond to this work with the potential parameters reported in table 2. (Colour in online version)

Table 3. Reference data used in our optimisation procedure.

Reference data	*Experimental value*
ρ_0 (kg m^{-3})	1137 [21]
ΔH_{vap} (kJ mol^{-1})	38.271 [22]
$P_{1st\ shock}$ (GPa)	7.54 [28]

3. Optimization method and results

3.1. Error criterion and reference database

Parameter optimizations are usually performed by minimizing an error function which represents the differences between reference data (experimental measurements or *ab initio* results) and data calculated with a given set of parameters. A simple form is the following:

$$F = \sum_{i=1}^{N} p_i \left| \frac{f_i - f_i^{ref}}{f_i^{ref}} \right|$$

where N is the number of reference data, f_i^{ref} is the i-th reference data, f_i is the calculated data and p_i is the relative weight of the property i with respect to the error function. The different f_i are computed simultaneously using parallelized routines.

In the case of nitromethane, only the repulsive and dispersive parameters have to be optimized since the electrostatic part has already been optimized. Three global reference data are used in this process. The two first reference data introduced in the error function F are the density (ρ_0) [21] and the vaporization enthalpy (ΔH_{vap}) [22] of liquid nitromethane at 298 K and 1 atm. These conditions correspond to the initial state of the Hugoniot. The third reference data is the pressure in a shock state ($P_{1st\ shock}$) of the Hugoniot ($V/V_0 = 0.6169$) obtained by Crouzet [28]. The target values are reported in table 3 and the error function F used in the case of nitromethane (details about F are given in the next paragraph) is reported in equation (10).

$$F = \frac{3}{8}\left|\frac{\rho_0^{calc} - \rho_0^{ref}}{\rho_0^{ref}}\right| + \frac{3}{8}\left|\frac{\Delta H_{vap}^{calc} - \Delta H_{vap}^{ref}}{\Delta H_{vap}^{ref}}\right| + \frac{1}{4}\left|\frac{P_{1^{st}shock}^{calc} - P_{1^{st}shock}^{ref}}{P_{1^{st}shock}^{ref}}\right| \quad (10)$$

Table 4. Experimental and simulated (with the initial parameters) properties of the nitromethane corresponding to the error function F.

Reference data	*Experimental value*	*Simulation value*	*Difference (%)*
ρ_0 (kg m^{-3})	1137 [21]	1135 ± 3	0.2
ΔH_{vap} (kJ mol^{-1})	38.271 [22]	37.34 ± 0.09	2.4
$P_{1st\ shock}$ (GPa)	7.54 [28]	10.55 ± 0.06	39.9

The data corresponding to the error function F computed with the initial parameter set are reported in table 4.

Unfortunately, computing the Hugoniot curve requires the knowledge of the initial state, namely the specific volume V_0, the pressure P_0 and the energy U_0, which depend themselves on potential parameters. Thus, the optimization of the initial state and the shock state cannot be perform simultaneously and should rather be done sequentially. The properties of the initial state should be computed prior to those of the shock state. Such a sequential route of optimization appears time consuming. To circumvent this problem, in the simulation of the first shock of the Hugoniot, we choose the initial state properties as equal to experimental values. As a consequence, if the error function on the properties of the initial state is relatively high, the calculation of the Hugoniot will not be significative. On the contrary, if the error function on the properties of the initial state is low, the calculation of the Hugoniot will be realistic. As the initial state is crucial in the determination of the Hugoniot curve, we decided to give a 75%-weight to the initial state in the error function. This imposes to have a parameter set that reproduces correctly the initial state. At the end of the optimization, an additional simulation of the Hugoniot with the real initial state properties (obtained with the current parameter set) is performed. In this way, obtaining slight differences between the results of the optimization and the exact simulation validates the whole procedure.

3.2. Stochastic exploration

An optimization problem may be solved using a minimization routine like for example the steepest descent method (Powell method) [6]. The total time necessary to complete the minimization process obviously depends on the details of the function to minimize. In our case, this corresponds to a thousand evaluations of the error function. Moreover this method leads to the local minimum of the function, and there is no guarantee that this minimum corresponds to the global minimum. In fact, this method is well suited for simple surface, i.e. when the function exhibits a small number of minima. Unfortunately, the shape of the surface is not known. The rugosity of the surface could be high and display a bunch of minima close from each other and with similar depths. To reach the global minimum, one would have to make an important number of minimizations with starting points dispatched over the whole parameter surface. This systematic investigation becomes rapidly time consuming as the number of parameters to optimize increases. As an example, a systematic investigation of a function of ten parameters, each parameter having 10 possible values would require 10^{10} evaluations of the error function. In order to investigate the behavior of the error function in the parameter space, we rather perform an exploration of this function in a Monte Carlo fashion. This allows to jump back and forth barriers, and eventually to reach the

global minimum. The conceptual difference between a local minimization and a random exploration is provided in figure 3. In our case, one evaluation of the error function takes few hours because it requires an entire *NPT* or *NVT* simulation. In this context, a simple minimization procedure could not be envisaged.

During the exploration, the parameter sets are chosen randomly (within physically bounded ranges: $50 < \varepsilon < 120\,\mathrm{K}$, $2 < \sigma < 5\,\text{Å}$, $11 < \alpha < 16$) and accepted with respect to the Metropolis criterion and the acceptance probability is:

$$P_{\mathrm{acc}}(\mathrm{old} \rightarrow \mathrm{new}) = \min\left\{1, \mathrm{e}^{\left(-\frac{f_{\mathrm{new}} - f_{\mathrm{old}}}{T^*}\right)}\right\}$$

where f_{new} is the error criterion calculated with the selected parameter set and f_{old} is the error criterion calculated with the previous parameter set. T^* is an indicator of the way we will accept parameter sets for which the f_{new} value is upper than f_{old}, this factor can be considered as a temperature (in the sense that it is related to the transition probability). For example, if T^* is fixed to 0.0217, it means that there is 10% probability to accept a parameter set which leads to an error function 5% higher than the error function obtained with the old parameter set.

At the end of the exploration, a population of parameters set is extracted. They can eventually be gathered in different groups, each of which corresponding to a value of the error function. A subsequent minimization could then be performed to reach the local minimum in each basin. This minimization has not been performed in our case for CPU time reasons. The stochastic exploration of the error function surface then appears determinant in the case of a complex minimization.

The method described here is rather simple but provides satisfactory results. If the optimization fails, other methods such as a J-walking Monte Carlo method [32] can succeed.

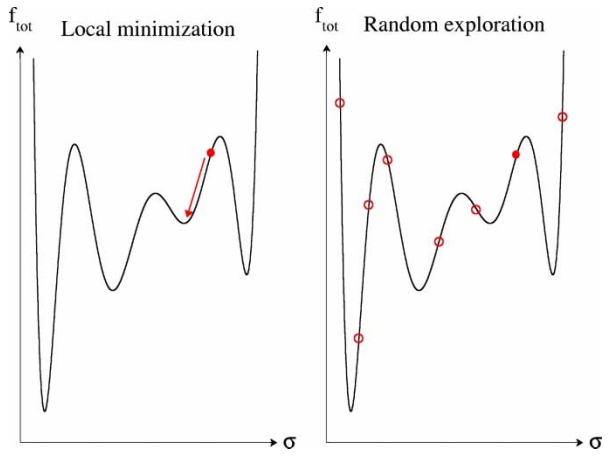

Figure 3. Comparison between a local minimization and a random exploration. The starting point of the optimization of a parameter σ is marked by a red dot. The path followed by the local minimization routine is symbolized by a red arrow. The red circles correspond to the points of the surface of parameters visited by the random exploration.

3.3. Optimization process

In this study, we have only optimized the ε, σ and α parameters of the exp-6 form since the electrostatic part of the potential has already been optimized. At the end of the optimization process, we checked that the initial state is always accurately described, the error functions on ρ_0 and ΔH_{vap} are lower than 10%.

More than 500 parameter sets have been evaluated. Particular attention has been given to the 20 parameter sets corresponding to the lowest error function. These sets can be grouped in three different basins, which are localized in close regions of the parameter surface. The average error function of the first group (6 sets) is around 2 and 4% for the last two groups (4 and 10 sets). Moreover, the minima belonging to the first basin reproduce better the initial state. This is the reason why we chose the parameter set with the lowest error function in this group as our optimized potential. The values of the parameters of the optimized potential are reported in table 5.

Other parameter sets belonging to the two other wells have been studied. For these parameter sets, the description of the initial state is less accurate. As a consequence, the Hugoniot curves obtained with these parameter sets do not show any improvement compared to the Hugoniot curve obtained with the initial parameter set.

3.4. Hugoniot properties of nitromethane with the optimized potential and properties of re-shocked nitromethane

As mentioned in paragraph 3.1, the Hugoniot is simulated with the experimental data of the initial state in the optimization procedure. A slight difference is observed when the Hugoniot is simulated with the exact data of the initial state (data obtained by the simulation of the initial state). Once the optimized potential is obtained, a check has been done on the initial state and the Hugoniot curve has been calculated with the exact data of the initial state. The density is $1144 \pm 3\,\mathrm{kg\,m^{-3}}$ and the vaporization enthalpy is $36.59 \pm 0.09\,\mathrm{kJ\,mol^{-1}}$. These quantities are consistent with those available at the end of the optimization. The whole Hugoniot curve is reported in figure 4. The Hugoniot curve is in very good agreement with experimental data. The pressure calculated at the first shock is $8.15 \pm 0.02\,\mathrm{GPa}$. The error function on $P_{1\mathrm{st\ shock}}$ is only 8.1% with the data of Crouzet, a difference comparable to the experimental error bars. Shock temperatures obtained with the optimized potential are reported in figure 5 and compared to previous curves. No major discrepancy is observed and results are in good

Table 5. Optimized potential parameters of nitromethane.

	σ (Å)	ϵ (K)	α
N	3.28714	59.3182	15.0766
O	2.79701	95.4856	12.4018
M	4.53075	99.1565	13.1211

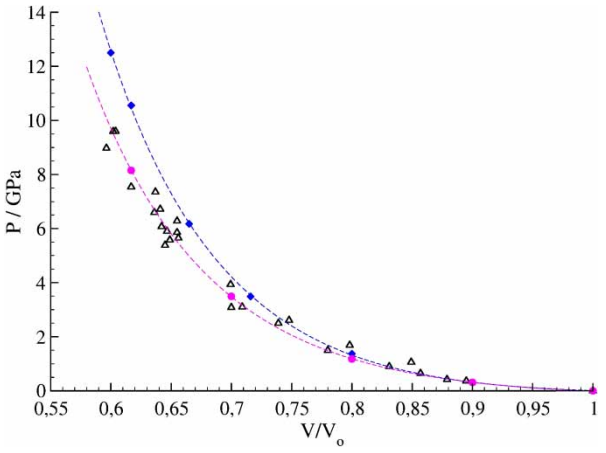

Figure 4. Hugoniot curves of nitromethane. Open triangles correspond to experimental data of Crouzet [28], Marsh [29], Klébert [30] and Craig [31]. Full symbols are results of simulations. Blue losanges: initial parameter set, pink dots: optimized parameter set. Dashed lines are a guide to the eyes. (Colour in online version)

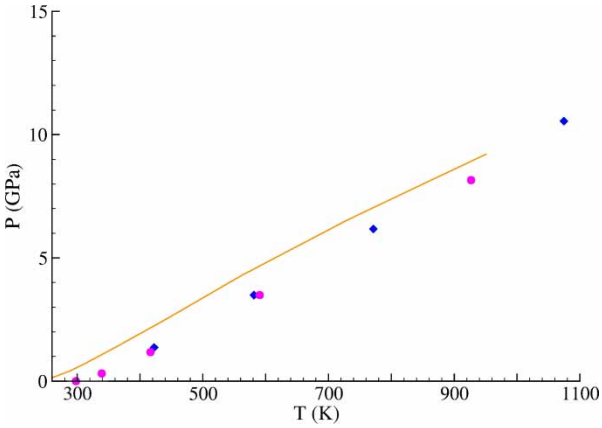

Figure 5. Pressure vs. temperature for the shock Hugoniot of nitromethane. Orange line: Lysne and Hardesty [1], blue losanges: initial parameter set, pink dots: optimized potential. (Colour in online version)

agreement with Lysne and Hardesty's one. The $u_s(u_p)$ curve is also very close to the experimental data. The quantities obtained with the initial parameter set and the optimized parameter set are summarized in table 6 together with experimental quantities.

After the compression, the material is in a particular state defined by the Hugoniot. When a second shock wave goes through the material (for example a reflected shock wave), the properties of the re-shocked material can still be obtained by the Rankine–Hugoniot relations. The accurate determination of the properties of re-shocked materials is very dependent of the quality of the force field used because the small discrepancies observed on the Hugoniot are magnified on the re-shocked Hugoniot. Moreover, a direct measurement of temperature is possible on the second Hugoniot.

The new potential has been optimized on the density and the energy of the initial state and on the pressure of the first shock. Other properties of the first shock are well reproduced, such as the shock temperature. The transferability of this new potential has been tested on re-shocked nitromethane properties. The comparison between experimental data on the reflected shock provided by Crouzet in our laboratory [28] and our simulation results is reported in table 7. The simulation results are in very good agreement with experimental data, especially for the shock temperature. It is important to note that, to our knowledge, no other potential is able to accurately reproduce shock temperatures and even more the second shock temperatures. As a consequence, the shock temperature appears relevant to evaluate the quality of a potential. Moreover, the computation of accurate shock temperatures is important for thermally activated processes, like chemical reactions.

It is important to remember that the optimized potential has been obtained during a random exploration of the parameters space. This parameter set is probably not the global minimum of the surface. To reach this minimum a minimization procedure should be performed. Nevertheless, in our case, results obtained with the optimized potential are sufficiently accurate and a minimization is not required.

Table 6. Experimental and simulated properties of nitromethane in initial state and shocked state.

Reference data	*Experiments*	*Initial potential*	*Optimized potential*
ρ_0 (kg m^{-3})	1137 [21]	1135 ± 3	1144 ± 3
ΔH_{vap} (kJ mol^{-1})	38.271 [22]	37.34 ± 0.09	36.59 ± 0.09
$P_{2nd\ shock}$ (GPa)	7.54 [28]	10.55 ± 0.06	8.15 ± 0.02
u_s (m s^{-1})	1587 [28]	1887 ± 8	1652 ± 4

3.5. Structural properties of nitromethane along the Hugoniot

In order to quantify the changes in structural properties of shocked nitromethane as density increases, CH_3–CH_3, CH_3–N, N–N, N–O and O–O radial distribution functions (RDF) have been calculated. The RDF shapes at ambient condition are similar to those of Liu *et al.* [16], Sorescu *et al.* [4] and Politzer's group [3,33]. The first neighbor shell around a nitromethane molecule is between 4 and 6 Å while the second shell is between 8 and 10 Å. From the RDF, the coordination number of nitromethane can be calculated as the integral of the first peak from zero to the first minimum. The coordination number reported for the first shell by Sorescu *et al.* [4] is 12.8, compared to 13.3 with our optimized potential.

We studied the evolution of the RDF as a function of pressure along the Hugoniot. Only the CH_3–CH_3 RDF is detailed here in figure 6. For the first shell, the single broad peak at 1 atm splits progressively in two peaks as pressure increases. This marks a progressive appearance of a structure in the fluid at high pressures. This phenomenon seems to be continuous up to 30 GPa where the first peak

Table 7. Experimental and simulated properties of the re-shocked nitromethane.

Reference data	*Experiments [28]*	*Initial potential*	*Optimized potential*
$P_{2nd\ shock}$ (GPa)	14.6	21.42 ± 0.05	16.13 ± 0.04
u_s (m s^{-1})	875	1035 ± 13	925 ± 7
T (K)	980 ± 50	1233	1057

appears at 3 Å while the second peak appears at 5 Å. At high pressures, the coordination number obtained by integration of these two peaks is 15. Integration of the first peak only gives 6 molecules and the second peak corresponds to 9 molecules. Due to compression under high pressure, the distance between a molecule and its first solvation shell usually decreases. As a consequence, in the RDF, the peak of the first shell shifts to the left. In order to distinguish the two peaks and reveal distance changes in excess to what is expected from the change in density, the RDF have been rescaled with respect to density (i.e. $r \rightarrow r(\rho/\rho_0)^{1/3}$ where ρ is the density at the considered pressure and ρ_0 is the density at ambient pressure). That is, for a group with distances decreasing in proportion to the density increase, no shift is expected. To a rigid structure of neighbors, the RDF peak would shift to the right whereas soft structure would lead to a shift to the left. The rescaled RDF are reported in figure 7. The shifting of the two peaks clearly show that the behavior of the first shell is dual. One part of the first shell behaves as a rigid structure whereas a second part behaves as a soft structure. In order to get information about the orientation of the molecules (not given by RDF), we have calculated the angle distribution of the total dipole of the molecules (see equation (11)) as done by Sorescu *et al.* on liquid nitromethane [4].

$$\langle \cos(\theta(r)) \rangle = \left\langle \frac{\vec{\mu}_i \vec{\mu}_j}{\mu^2} \right\rangle \tag{11}$$

Our results at ambient pressure and temperature are in good agreement with those of Sorescu *et al*. At short distance separation (~3 Å), the most favorable configuration between two nitromethane molecules is antiparallel alignment of the dipoles. Above 4 Å, the alignment of the dipoles is roughly orthogonal ($\theta(r)$ contained between 70 and 110°). Under high pressure, no major differences can be seen. This shows that no specific alignment of the dipoles is observed. These results seem to indicate that nothing but a steric reorganization of nitromethane molecules occurs under high pressure.

4. Conclusion

In this work, the novel scheme proposed by Bourasseau and co-workers [6–8] for the optimization of classical potentials to describe atomic interactions has been applied to shocked nitromethane.

This approach is based on a sequential optimization process according to the separation of the total energy into three contributions. A logical order for the optimization is followed: first the intramolecular contribution, then the electrostatic one, and lastly the repulsive-dispersive part. In the case of nitromethane, the influence of the internal geometry of the molecules is negligible on the Hugoniot curve. As a consequence, the internal geometry of the molecules is kept rigid and the intramolecular energy is constant. The electrostatic part has previously been optimized by Bourasseau *et al.* [6,7]. The present work focuses on the optimization of the repulsive-dispersive part.

In order to optimize parameters of a potential, the logical way is to minimize an error function with a steepest descent method. Nonetheless, this method has two main drawbacks: the minimum reached depends on the starting point and the computation time isdependent of the time needed to evaluate the error function. In the case of nitromethane, nine parameters are optimized. As a consequence, the

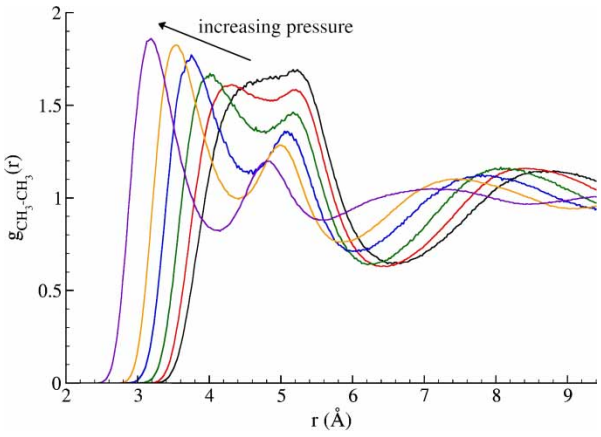

Figure 6. CH_3–CH_3 RDF at six different pressures (black, 1 atm; red, 0.313 GPa; green, 1.18 GPa; blue, 3.49 GPa; orange, 8.15 GPa; violet, 28.43 GPa) along the Hugoniot from AE-EOS *NV*Hug simulations. (Colour in online version)

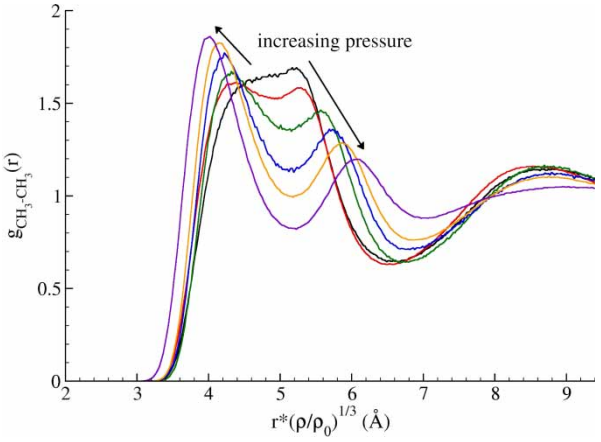

Figure 7. CH_3–CH_3 RDF at six different pressures (black, 1 atm; red, 0.313 GPa; green, 1.18 GPa; blue, 3.49 GPa; orange, 8.15 GPa; violet, 28.43 GPa) along the Hugoniot from AE-EOS *NV*Hug simulations. Distances are rescaled to ambiant density. (Colour in online version)

rugosity of the parameter surface is probably high and displays many minima close to each other and with similar depths. Moreover, one evaluation of the error function requires an entire *NPT* or *NVT* simulation (few hours). In this context, a minimization procedure appears impractical. Instead of minimizing an error function to reach the closest local minimum, an exploration of the surface of parameters is performed by a random way. Parameter sets are accepted with respect to a Metropolis criterion. At the end of the exploration, a population of parameter sets is extracted and gathered in different groups.

In this paper, we optimized the repulsion–dispersion parameters of nitromethane on the density and the vaporization enthalpy of the initial state (the pole of the Hugoniot) and on one value of experimental pressure along the Hugoniot. Our results clearly show that an adequate functional form (exp-6) for the repulsion–dispersion interaction, point charges and a rigid molecule can predict accurate quantities along the Hugoniot. The properties of shocked nitromethane are accurately reproduced with the optimized potential. Moreover, a good accuracy is also observed on second shock properties. The shock temperature is seen to be a discriminating quantity to reveal the quality of the force field. Our potential can predict the second shock temperature with 8% difference to experimental data. This accuracy has to be compared with the 5% experimentaluncertainty and the poor accuracy of other published potentials.

In a second stage, structural properties of shocked nitromethane have been studied. As pressure increases, a progressive structuration of the fluid seems to occur. The low density first shell splits in two separate groups. A first group behaves as a rigidstructure whereas the second group behaves as a soft structure. No particular information can be extracted from angular distributions and no specific alignment of molecules is observed. A steric reorganization seems to occur under high pressures.

To conclude, the optimization method described in [6–8] has been improved and applied to nitromethane. The method appears well suited for the construction of transferable and accurate potential over a large range of thermodynamic conditions. The force field obtained for nitromethane is in very good agreement with experimental data for shocked and re-shocked nitromethane.

Acknowledgements

I.F.P., C.N.R.S. and the Université Paris-Sud are gratefully acknowledged for providing us the Gibbs molecular simulation code, used to perform the Monte Carlo simulations.

References

[1] P.C. Lysne, R.D. Hardesty. Fundamental equation of state of liquid nitromethane to 100 kbar. *J. Chem. Phys.*, **59**, 6512 (1973).

[2] N.C. Blais, R. Engelke, S.A. Sheffield. Mass spectroscopic study of the chemical reaction zone in detonating liquid nitromethane. *J. Phys. Chem.*, **101**, 8285 (1997).

[3] J.M. Seminario, M.C. Concha, P. Politzer. A density-functional molecular-dynamics study of the structure of liquid nitromethane. *J. Chem. Phys.*, **102**, 8281 (1995).

[4] D.C. Sorescu, B.M. Rice, D.L. Thompson. Molecular dynamics simulations of liquid nitromethane. *J. Phys. Chem. A*, **105**, 9336 (2001).

[5] M.R. Manaa, E.J. Reed, L.E. Fried, G. Galli, F. Gygi. Early chemistry in hot and dense nitromethane: Molecular dynamics simulations. *J. Chem. Phys.*, **120**, 10146 (2004).

[6] E. Bourasseau, J.-B. Maillet, L. Mondelain, P.-M. Anglade. New potential model for molecular dynamic simulation of liquid HF. I—Parameter optimization for charge equilibration method. *Mol. Simul.*, **31**, 705 (2005).

[7] E. Bourasseau, J.-B. Maillet. APS shock compression of condensed matter. p. 565 (2005)

[8] V. Dubois, E. Bourasseau, J.-B. Maillet. New potential model for molecular dynamic simulation of liquid HF. II—Parameter optimization for repulsion-dispersion potential. *Mol. Phys.*, **105**, 125 (2007).

[9] E. Bourasseau, M. Haboudou, A. Boutin, A.H. Fuchs, P. Ungerer. New optimization method for intermolecular potentials: Optimization of a new anisotropic united atoms potential for olefins: Prediction of equilibrium properties. *J. Chem. Phys.*, **118**, 3020 (2003).

[10] W. Mortier, S. Gosh, S. Shankar. Electronegativity equalization method for the calculation of atomic charges in molecules. *J. Am. Chem. Soc.*, **108**, 4315 (1986).

[11] A. Rappé, W. Goddard. Charge equilibration for molecular-dynamics simulations. *J. Chem. Phys.*, **95**, 3358 (1991).

[12] S. Rick, S. Stuart, B. Berne. Dynamic fluctuating charge force-fields—Application to liquid water. *J. Chem. Phys.*, **101**, 6141 (1994).

[13] H. Liu, J. Zhao, D. Wei, Z. Gong. Structural and vibrational properties of solid nitromethane under high pressure by density functional theory. *J. Chem. Phys.*, **124**, 124501 (2006).

[14] M.L.P. Price, D. Ostrovsky, W.L. Jorgensen. Gas-phase and liquid-state properties of esters, nitriles, and nitro compounds with the OPLS-AA force field. *J. Comp. Chem.*, **22**, 1340 (2001).

[15] P. Ungerer, C. Beauvais, J. Delhommelle, A. Boutin, B. Rousseau, A.H. Fuchs. Optimization of the anisotropic united atoms intermolecular potential for n-alkanes. *J. Chem. Phys.*, **112**, 5499 (2000).

[16] H. Liu, J. Zhao, G. Ji, Z. Gong, D. Wei. Compressibility of liquid nitromethane in the high-pressure regime. *Phys. B*, **382**, 334 (2006).

[17] F. Saija, S. Prestipino. High-pressure phase diagram of the exp-6 model: The case of Xe. Issue of the article : 2, Number of the article : 024113. *Phys. Rev. B*, **72** (2005).

[18] M. Ross. *High Pressure Chemistry and Biochemistry*, Reidel, Dordrecht (1987).

[19] E. Bourasseau. Prédiction des propriétés d'équilibre de phases par simulation moléculaire. PhD Thesis, Université Paris-Sud XI (2003)

[20] D.C. Sorescu, B.M. Rice, D.L. Thompson. Intermolecular potential for the hexahydro-1,3,5-trinitro-1,3,5-s-triazine crystal (RDX): A crystal packing, Monte Carlo, and molecular dynamics study. *J. Phys. Chem.*, **101**, 798 (1997).

[21] D.R. Lide. *Handbook of Chemistry and Physics*, CRC Press, Boca Raton (1997).

[22] W.M. Jones, W.F. Giauque. The Entropy of Nitromethane. Heat Capacity of Solid and Liquid. Vapor Pressure, Heats of Fusion and Vaporization. *J. Am. Chem. Soc.*, **69**, 983 (1947).

[23] J. Brennan, B. Rice. Efficient determination of Hugoniot states using classical molecular simulation techniques. *Mol. Phys.*, **101**, 3309 (2003).

[24] A. Hervouët, N. Desbiens, E. Bourasseau, J.-B. Maillet. Microscopic approaches to liquid nitromethane detonation properties, in preparation (2007).

[25] E. Bourasseau, V. Dubois, N. Desbiens, J.-B. Maillet. Molecular simulations of Hugoniots of detonation products mixtures at chemical equilibrium: microscopic calculation of the Chapman–Jouguet state. *J. Chem. Phys.* (2007).

[26] H.D. Jones. APS shock compression of condensed matter. p. 149 (2003)

[27] L. Soulard. APS shock compression of condensed matter. p. 173 (2001)

[28] B. Crouzet, D. Partouche-Sebban, N. Carion. APS shock compression of condensed matter. p. 1253 (2003)

[29] S.P. Marsh. *LASL Shock Hugoniot Data*, p. 1980, University of California, Berkeley (1980).

[30] P. Klébert. Etude expérimentale et théorique de la transition choc détonation dans les explosifs homogènes. PhD Thesis, Paris VI—Pierre et Marie Curie University (1998).

[31] B.G. Craig. Los Alamos Scientific Laboratory Report Number GMX-8-MR-62-4 (1962).

[32] D. Frantz, D. Freeman, J. Doll. Reducing quasi-ergodic behavior in Monte-Carlo simulations by J-Walking—Applications to atomic clusters. *J. Chem. Phys.*, **93**, 2769 (1990).

[33] H.E. Alper, F. Abu-Awwad, P. Politzer. Molecular dynamics simulations of liquid nitromethane. *J. Phys. Chem. B*, **103**, 9738 (1999).